^{19}F-NMR Spin–Spin Relaxation (T_2) Method for Characterizing Volatile Anesthetic Binding to Proteins. Analysis of Isoflurane Binding to Serum Albumin†

Brian W. Dubois and Alex S. Evers*

Departments of Anesthesiology and Molecular Biology & Pharmacology, Washington University School of Medicine, St. Louis, Missouri 63110

Received March 23, 1992; Revised Manuscript Received May 14, 1992

ABSTRACT: This paper characterizes the low-affinity ligand binding interactions of a fluorinated volatile anesthetic, isoflurane ($CHF_2OCHClCF_3$), with bovine serum albumin (BSA) using ^{19}F-NMR transverse relaxation (T_2). ^{19}F-NMR spectra of isoflurane in aqueous BSA reveal a single isoflurane trifluoromethyl resonance, indicative of rapid exchange of isoflurane between protein-bound and aqueous (free) environments. The exchange is slow enough, however, that the chemical shift difference between bound and free isoflurane ($\delta\omega$ = 0.545 ppm) contributes to the observed isoflurane T_2. The contribution of $\delta\omega$ to T_2 can be minimized by shortening the interval between 180° refocusing pulses in the Carr–Purcell–Meiboom–Gill pulse sequence used to monitor T_2. Analysis of the dependence of T_2 on interpulse interval additionally allows determination of the T_2 (6.2 ms) and the average lifetime (τ_b = 187 μs) of bound isoflurane molecules. By use of a short interpulse interval (<100 μs), T_2 measurements can readily be used to analyze equilibrium binding of isoflurane to BSA. This analysis revealed a discrete saturable binding component with a K_D = 1.4 mM that was eliminated either by coincubation with oleic acid (6 mol/mol of BSA) or by conversion of BSA to its "expanded" form by titration to pH 2.5. The binding was independently characterized using a gas chromatographic partition analysis (K_D = 1.4 mM, B_{max} = 3–4 sites). In summary, this paper describes a method whereby T_2 measurements can be used to characterize equilibrium binding of low-affinity ligands to proteins without the confounding contributions of chemical shift. Additionally, this paper *directly* demonstrates that distinct volatile anesthetic binding sites exist on certain proteins, in certain conformations, and provides a sensitive method to study them.

The well-known correlation between general anesthetic potency and lipid solubility has been interpreted to suggest that the primary target sites for these agents are the lipid matrices of biological membranes. The alternative view that hydrophobic sites on sensitive target proteins are the primary molecular targets for general anesthetics has also been proposed (Franks & Lieb, 1984; Richards et al., 1978). There are several lines of indirect evidence in favor of direct protein interactions. For example, discrete binding has been suggested by the observation that optical isomers of isoflurane ($CHF_2OCHClCF_3$) display stereospecific effects on the function of certain neuronal ion channels (Franks & Lieb, 1991). Furthermore, the anesthesia "cutoff" effect has been interpreted to suggest that anesthetic target sites have definite molecular dimensions: *n*-Alkanes and *n*-alkanols increase in anesthetic potency with increasing chain length until they reach a critical length, at which anesthetic potency abruptly disappears (Alifimoff et al., 1989). The association of the in vivo cutoff effect with protein binding is strengthened by the observation that the anesthetic inhibition of firefly luciferase, a water-soluble enzyme, also displays an anesthetic cutoff effect (Franks & Lieb, 1987).

Volatile anesthetics have also been shown to directly alter protein structure. High anesthetic concentrations produce broad perturbations of hemoglobin and serum albumin structure, as assessed by circular dichroism and optical rotatory dispersion (Balasubramanian & Wetleufer, 1966; Laasberg & Hedley-Whyte, 1971). More specific perturbations of hemoglobin structure have been observed at lower anesthetic concentrations, using high-resolution proton NMR spectroscopy (Brown et al., 1976). It is uncertain that these perturbations reflect discrete volatile anesthetic binding to specific sites on the proteins. In fact, there is evidence to the contrary to suggest that volatile anesthetics interact without specificity at most protein–water interfacial surfaces (Mashimo et al., 1986).

Unfortunately, little *direct* evidence exists to demonstrate, or characterize, volatile anesthetic binding to discrete sites on proteins. In this study we have utilized ^{19}F-NMR spectroscopy to directly observe and characterize fluorinated volatile anesthetic binding to purified proteins. ^{19}F NMR was used because fluorinated volatile anesthetics can be easily observed against a silent background, and because the large magnetogyric ratio of ^{19}F offers a relatively high sensitivity. The NMR analysis takes advantage of the fact that anesthetic molecules rapidly exchange between protein-bound and aqueous free states. The rapid exchange results in a single observable anesthetic NMR signal that contains information concerning both the bound and free states. Particular emphasis is given to an analysis of the spin–spin (T_2) behavior (Fischer & Jardetsky, 1965; Schmidt et al., 1969) of the exchanging system in order to determine the anesthetic equilibrium binding constant (K_D) and the rate of anesthetic exchange. In this study, equilibrium anesthetic binding is also characterized by analysis of ^{19}F-NMR chemical shift (Dwek, 1975), an approach that requires much larger amounts of protein.

Albumin was initially studied because its availability in large quantity permitted a gas chromatographic partition analysis to independently corroborate the measured equilibrium binding constant. Albumin was expected to interact with volatile anesthetics on the basis of previous evidence of

† This work was supported by NIH Grant RO1 GM37846 (A.S.E.). A.S.E. is an established investigator of the American Heart Association.

* Author to whom correspondence should be addressed: Washington University School of Medicine, Department of Anesthesiology Research, Box 8054, 660 South Euclid Ave., St. Louis, MO 63110.

0006-2960/92/0431-7069$03.00/0

hydrocarbon–BSA interactions (Wishnia & Pinder, 1964) and evidence that BSA increased volatile anesthetic partitioning into plasma (Laasberg & Hedley-Whyte, 1970). In addition, the structures of the various ligand binding sites on albumin are becoming increasingly defined. Consequently, volatile anesthetic binding to defined sites could be amenable to pharmacologic analysis using site-specific competitive ligands.

In an attempt to demonstrate specificity of volatile anesthetic–macromolecule interactions, anesthetic binding to lysozyme, and poly(L-lysine), was also examined. Lysozyme was not expected to bind volatile anesthetics on the basis of evidence of minimal interactions with hydrocarbons (Wishnia, 1962). Poly(L-lysine) (114 kDa), which is very highly charged at pH 7.2, was also not expected to offer suitable environments for anesthetic binding.

MATERIALS AND METHODS

Materials. Lyophilized bovine serum albumin (fraction V, fatty acid free, purity >96% by electrophoresis) was purchased from Calbiochem (La Jolla, CA). Lyophilized poly(L-lysine) hydrobromide (molecular mass 114 kDa), crystalline lysozyme (from chicken egg white), and sodium oleate were purchased from Sigma (St. Louis, MO). Isoflurane (as a racemic mixture of isoflurane isomers) was obtained from Anaquest (Madison, WI).

Methods. Preparation of Protein Solutions. Lyophilized proteins were dissolved by gentle magnetic stirring into a 5 mM sodium Hepes buffer solution (pH 7.4) containing 135 mM KCl, 15 mM sodium gluconate, 1 mM EDTA, 0.75 mM $CaCl_2$, and 10 mM glucose.[1] Gas chromatographic partition studies were performed using BSA (MW 66 200) at high concentrations, 27.8–100 mg/mL (0.420–1.51 mM). BSA solutions for ^{19}F-NMR T_2 measurements were made at significantly lower concentrations, with a range of 0.75–6.0 mg/mL (11.3–90.6 μM). All NMR samples were prepared to contain 20% D_2O for use as a lock and shim signal.

Preparation of Fatty Acid–Albumin Solutions. Oleic acid was complexed to BSA as described by Spector (1986). Briefly, a measured amount of sodium oleate was dissolved in hexane slightly alkalinized with 1 M NaOH. The hexane was evaporated under N_2 and the oleate redissolved in distilled water. The aqueous oleic acid was then added to a given amount of BSA, so that the final oleic acid/BSA molar ratio was known. The final solution pH was verified to be 7.4. Molar ratios ranging from 1.5 to 12.0 were prepared.

Equilibration and Gas Chromatographic Techniques. Samples (4 mL) of either protein solution or buffer were separately injected into different gas sampling bulbs (1 L) containing various concentrations (0.5–15 vol %) of volatilized isoflurane ($CHF_2OCHClCF_3$). The bulb valves were opened momentarily to ensure atmospheric pressure before beginning a 90-min sample equilibration period, at 22 °C. After equilibration, a gas-tight Hamilton syringe was used to withdraw a small (1 mL) gas sample from the bulbs, and a final gaseous anesthetic concentration was determined. This was performed by isothermal gas chromatography on a packed Porapak Q column using flame ionization detection (Heavner et al., 1976). The liquid sample (1 mL) was similarly withdrawn from the bulbs using a gas-tight syringe, and the anesthetic concentration was determined by organic extraction followed by capillary gas chromatography as previously described (Stern et al., 1989).

Equilibrium Binding Determination by Gas Chromatography. After equilibration with a given gaseous anesthetic concentration, buffer and protein solutions have identical free aqueous anesthetic concentrations. The protein solution has a total anesthetic concentration equal to the aqueous free anesthetic concentration plus the protein-bound anesthetic concentration. By subtracting the aqueous anesthetic concentration as measured by the buffer sample, $[VA_{buffer}]$, from the total protein solution anesthetic, $[VA_{total}]$, the protein-bound anesthetic concentration, $[VA_{bound}]$, can be determined. Since the protein volume in a 10–100 mg/mL solution is very small compared to the aqueous volume, the simple subtraction provides an excellent estimate of the bound anesthetic concentration. In this study, soluble protein was assumed to have a partial specific volume of 0.75, or a density of 1.33. Buffer was assumed to have a density of 1.0. The subtraction was modified to include the buffer correction for an x mg/mL protein solution

$$[VA_{bound}] = [VA_{total}] - ((1000 - 0.75x)/1000)[VA_{buffer}] \quad (1)$$

where $(1000 - 0.75x)/1000$ equals the volume fraction occupied by buffer in an x mg/mL protein solution. $[VA_{bound}]$ was measured over a range of protein concentrations, and over a range of gas concentrations, in order to generate an anesthetic equilibrium binding isotherm. The bound isoflurane was expressed in terms of moles of isoflurane bound per mole of protein and plotted as a function of buffer isoflurane concentration, $[VA_{buffer}]$.

Isoflurane equilibrium binding to BSA was also examined in the presence of oleic acid, a long-chain fatty acid and endogenous high-affinity ligand for albumin. Since oleic acid binds with very high affinity to BSA, oleic acid becomes largely protein bound in fatty acid–albumin solutions, provided that the molar ratio of oleic acid/BSA is kept reasonably low. The free aqueous isoflurane concentration in a fatty acid–albumin solution is consequently assumed to be similar to buffer. Bound anesthetic is determined by subtracting the aqueous anesthetic concentration as measured by the buffer sample from the total fatty acid–albumin solution anesthetic concentration.

^{19}F-NMR Methodology. Solutions were equilibrated in gas sampling bulbs with volatilized isoflurane as described above. Final equilibrium gas concentrations, measured by gas chromatography, were used to calculate aqueous isoflurane concentrations in the samples, based on the experimentally determined partition coefficient. A gas-tight syringe was used to transfer samples into 5-mm NMR tubes, which were capped immediately. These tubes were filled almost completely to avoid volatile anesthetic loss from the liquid phase. Volatile anesthetic escape from the sealed NMR tubes was negligible, as all ^{19}F-NMR measurements could be reproducibly obtained days afterward.

^{19}F-NMR measurements were obtained on a Varian VXR-500 multinuclear spectrometer operating at 470.3 Mhz. Experiments were temperature controlled at 22 °C, unless otherwise indicated, with internal D_2O serving as both a lock and shim signal. Trifluoroacetic acid in an external capillary served as a chemical shift reference.

Spin–spin relaxation (T_2) measurements were obtained using the Carr–Purcell–Meiboom–Gill (CPMG) pulse sequence (Meiboom & Gill, 1958). A nonselective 90° pulse (t_{90} = 9 μs) was used to excite the sample, and multiple non-

[1] Isoflurane binding to BSA was additionally examined in phosphate-buffered saline (116 mM NaCl, 4.9 mM KCl, 1.2 mM $MgSO_4$, and 16 mM sodium phosphate, pH 7.4). The T_2 analysis revealed a similar discrete saturable binding component (K_D = 2.4 ± 0.3 mM) that was analogously eliminated by oleic acid (6 mol of oleic acid/mol of BSA).

selective 180° refocusing pulses (t_{180} = 18 μs) generated the echo train. The time between 180° refocusing pulses, τ_{cp}, varied from 4 ms to 80 μs (as explained in the T_2 theory section). The time between successive echo sequences was greater than 4 times T_1 to assure sample equilibrium. Relaxation data were collected for an interval spanning at least 2–3 times the T_2 decay constant. The data (four to eight transients) are plotted as a function of echo evolution time and fit to a single exponential using the NFITS nonlinear least squares fitting program (written by C. Lingle). T_2 values are reported as time constants of these exponentials.

NMR Transverse Relaxation (T_2) Theory. In a protein solution, anesthetic molecules can exchange between at least two different chemical environments: a bound state and an aqueous free state. The chemical environments are characterized by different chemical shifts, δ_b, and δ_f, respectively. If the chemical exchange rate between the two environments is slow compared to the chemical shift difference ($\delta\omega = \delta_b - \delta_f$), resonances at δ_b, and at δ_f, are in principle, observable. If the chemical exchange rate is fast with respect to the chemical shift difference, the two signals coalesce to ultimately form a single narrow feature (Dwek, 1973). Under the condition of complete coalescence into a single narrow resonance, the relaxation rate ($1/T_2$) equals the weighted average of the relaxation rates of the bound ($1/T_{2b}$) and free ($1/T_{2f}$) anesthetic. Here, the exchange rate far exceeds $\delta\omega$ and $1/T_{2b}$, and the observed relaxation rate ($1/T_2$), is simply expressed (Dwek, 1973)

$$1/T_2 = X_f/T_{2f} + X_b/(T_{2b} + \tau_b) \quad (2)$$

where X_f is the anesthetic mole fraction that is free, X_b is the anesthetic mole fraction that is bound ($X_f + X_b = 1$), and τ_b is the average lifetime in the bound state (which is usually much shorter than T_{2b}).

However, if the exchange rate is slow enough to cause line width broadening of the single resonance (incomplete coalescence), $1/T_2$ is better expressed (Swift & Connick, 1962)

$$1/T_2 = X_f/T_{2f} + X_b/\tau_b \frac{(1/T_{2b})^2 + 1/(T_{2b}\tau_b) + (\delta\omega)^2}{((1/T_{2b} + (1/\tau_b))^2 + (\delta\omega)^2} \quad (3)$$

There is an increase in the relaxation rate ($1/T_2$), or broadening of the line width, when the chemical shift difference is not negligibly small in relation to the exchange rate. Under these conditions, $1/T_2$, as measured by the CPMG sequence, varies as a function of the CPMG 180–180° interpulse space interval (τ_{cp}) (Carver & Richards, 1972). The relaxation rate ($1/T_2$) as a function of τ_{cp} is given (Luz & Meiboom, 1963; Allerhand & Gutowsky, 1965) by

$$1/T_2 = X_f/T_{2f} + X_b/(T_{2b} + \tau_b) + [\tau_b X_b X_f(\delta\omega)^2(1 - (2\tau_b/\tau_{cp}) \tanh (\tau_{cp}/2\tau_b))] \quad (4)$$

A plot of $1/T_2$ versus the CPMG pulsing rate ($1/\tau_{cp}$) results in a hyperbolic tangent. The upper and lower limits of the function represent useful, simplified cases for $1/T_2$. These limits can be appreciated by varying τ_{cp} in eq 4.

(*a*) *Slow Pulsing Limit.* An upper limit for the relaxation rate is approached when the interpulse space interval is long in comparison to the exchange rate ($\tau_{cp} \gg \tau_b$). Here, $1/T_2$ becomes equal to the Swift and Connick description, eq 3 (Carver & Richards, 1972; Hills et al., 1989).

(*b*) *Fast Pulsing Limit.* A lower limit for the relaxation rate is approached when the interpulse space interval becomes shorter than the lifetime bound ($\tau_{cp} < \tau_b$). In this case, the bracketed term in eq 4 approaches zero, and eq 4 reduces to eq 2 (Carver & Richards, 1972). With a fast CPMG pulsing rate, the contribution of chemical exchange is in effect removed from the relaxation rate (Carver & Richards, 1972; Gerig & Stock, 1975).

Mechanistically, the fast pulsing rate minimizes the time for exchange between the 180–180° pulses and, therefore, prevents a chemical exchange contribution to magnetic spin dephasing and, hence, transverse relaxation (Hills et al., 1990). This is analogous to the "spin-locking" technique where a continuous field is applied in place of the 180–180° pulsing train, effectively reducing the interpulse spacing to zero. In principle, the spin-locking technique can likewise be used to measure $1/T_2$ without the complication of chemical shift (Jackman & Cotton, 1975).

Spin-Locking Equivalent of the CPMG Sequence. The CPMG sequence, using a short interpulse space interval, is shown to be equivalent to a spin-locking sequence. Spin-locking experiments (Hartmaan & Hahn, 1962) were performed which consisted of a nonselective 90° pulse (t_{90} = 15 μs), immediately followed by a locking pulse of duration t_{sl}. Relaxation data were collected by sampling after various locking pulse durations. The relaxation data were fit to a single exponential exactly as described for the CPMG relaxation data. Two locking field frequencies of 3333 and 12 500 Hz were used. The locking field frequencies were converted to a CPMG 180–180° pulsing rate equivalent. The CPMG pulsing equivalent of a locking field of frequency, f, is given by $1/\tau_{cp} = 2f$ (Santyr et al., 1988).

Determination of τ_b by Varying the CPMG 180–180° Interpulse Space Interval. The dependence of $1/T_2$ on the pulsing rate ($1/\tau_{cp}$) permits the determination of τ_b by fitting to eq 4. This is done using the NFITS nonlinear least squares fitting program. Insertion of X_b and X_f, measured by gas chromatography, and T_{2f}, measured with buffer, allowed the additional fitting of $\delta\omega$ and T_{2b}. In theory, different values for X_b should yield similar determinations of τ_b, $\delta\omega$, and T_{2b}. The value $\delta\omega$, derived from the fit, is compared with the experimentally determined $\delta\omega$ derived in the results.

Equilibrium Binding Constant, K_D, by ^{19}F-NMR T_2 Analysis. The dependence of T_2 on anesthetic concentration is used to characterize anesthetic binding. A fast CPMG pulsing rate is used in measuring the relaxation rate, $1/T_2$. With a fast CPMG pulsing rate, $1/T_2$ is not complicated by chemical exchange and $1/T_2$ is simply described by eq 2. A single equilibrium binding process is illustrated

$$[A] + [R] \underset{k_{off}}{\overset{k_{on}}{\rightleftarrows}} [RA] \quad (5)$$

where [A] is the aqueous anesthetic concentration, [R] is the binding site concentration, [RA] is the bound anesthetic concentration, and $K_D = k_{off}/k_{on} = [R][A]/[RA]$. $X_b = [RA]/[A]$, provided that the free anesthetic concentration is in large excess over the bound anesthetic concentration. By inserting K_D and the expression for X_b into eq 2, one finds that eq 2 takes the form (Behling et al., 1988; Miller et al., 1979; Fraenkel et al., 1990)

$$T_{2p} = [A](T_{2b} + \tau_b)/[R] + K_D(T_{2b} + \tau_b)/[R] \quad (6)$$

where $T_{2p} = (1/T_2 - 1/T_{2f})^{-1}$. An X–Y plot of T_{2p} versus the anesthetic concentration, [A], has a slope of $(T_{2b} + \tau_b)/[R]$, and an x-intercept equal to $-K_D$. The linearity of the plot reaffirms the single equilibrium binding assumption. A value for $T_{2b} + \tau_b$ can be determined from the slope, using [R] measured by gas chromatographic partition measurements.

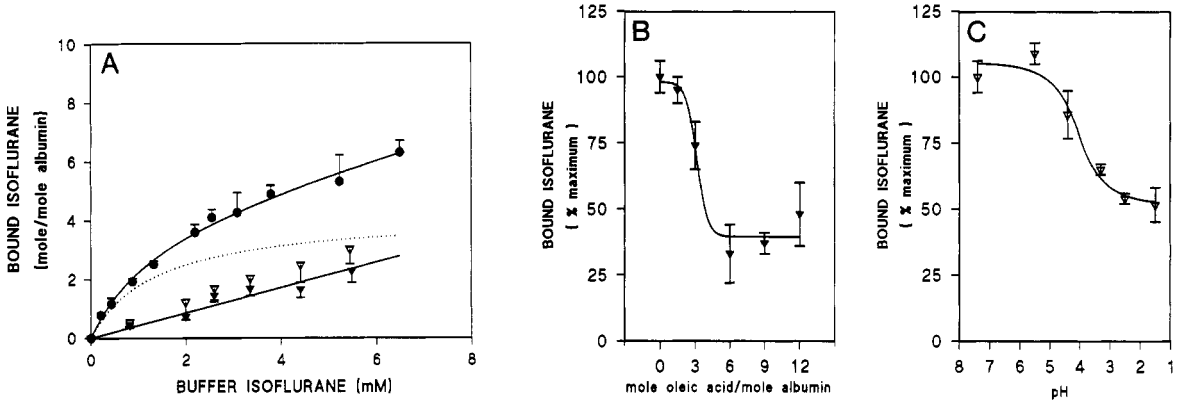

FIGURE 1: (A) Gas chromatographic partition analysis of isoflurane equilibrium binding to BSA at 22 °C, pH 7.2. BSA solutions (28 mg/mL) were equilibrated with gaseous isoflurane (0–15 vol %) to give aqueous concentrations indicated on the abcissa. Equilibrations were conducted in the presence (▼) or absence (●) of oleic acid (6:1 oleic acid/BSA mole ratio). Bound isoflurane was calculated by subtracting aqueous concentrations, as measured using buffer samples, from total solution isoflurane concentrations, according to eq 1. Isoflurane binding in the presence of oleic acid was subtracted from total isoflurane binding to more clearly define a higher affinity binding component (dotted line), K_D = 1.4 ± 0.2 mM, B_{max} = 4.2 ± 0.3 sites (n = 4, ±SD). Alternatively, isoflurane binding to BSA at pH 2.5 (▽) could be used to define the higher affinity binding component (not shown), K_D = 1.1 ± 0.2 mM, B_{max} = 3.3 ± 0.2 sites (n = 4, ±SD). (B) Partition analysis of isoflurane binding to BSA, at an aqueous isoflurane concentration of 4 mM, in the presence of oleic acid at molar ratios (oleic acid/BSA) ranging from 1.5 to 12.0. (C) Partition analysis of isoflurane binding to BSA, at an aqueous isoflurane concentration of 4.42 mM, as a function of pH.

RESULTS

Gas Chromatographic Analysis of Isoflurane Equilibrium Binding. Isoflurane equilibrium binding to BSA (fatty acid free) at 22 °C was characterized by separately incubating BSA solutions (27.8 mg/mL) and buffer with various concentrations of gaseous isoflurane (0.5–15 vol %). Initial experiments showed that complete equilibration between aqueous and gaseous phases occurred in less than 90 min, consistent with previous results (Laasberg & Hedley-Whyte, 1970). After releasing the bulb pressures, and allowing for the equilibration period, the gaseous isoflurane concentration was measured. Equilibrium gas concentrations were found to be identical in bulbs containing buffer and protein solutions and ranged from 0.50 ± 0.01% to 13.6 ± 0.4% (±SD). The resulting isoflurane buffer concentrations ranged from 0.23 ± 0.02 to 6.4 ± 0.2 mM, producing a uniform buffer–gas partition coefficient of 1.1 ± 0.08. This is in agreement with the published value of 1.08 (Firestone et al., 1986). The total isoflurane concentrations in BSA solutions were considerably higher and ranged from 0.54 ± 0.03 to 9.1 ± 0.3 mM. Bound isoflurane was calculated by subtracting buffer isoflurane from total BSA solution isoflurane, according to eq 1. The bound isoflurane was then converted to a mole bound per mole of albumin ratio using a BSA molecular mass of 66.2 kDa. Isoflurane binding was measured at several BSA concentrations to verify that the stoichiometry of isoflurane binding was not influenced by the BSA concentration. For example, BSA solutions of 27.8, 43.3, 71.6, and 100 mg/mL were equilibrated with 4.7% gaseous isoflurane (2.1 ± 0.2 mM aqueous free isoflurane) to yield total BSA solution isoflurane concentrations of 3.5 ± 0.2, 4.2 ± 0.1, 5.5 ± 0.2, and 6.3 ± 0.3 mM, respectively. The buffer concentration, 2.1 ± 0.1 mM, was subtracted according to eq 1, and bound isoflurane was found to be similar: 3.4, 3.3, 3.3, and 2.9 mol bound/mol of BSA.

Isoflurane binding to BSA (27.8 mg/mL) was plotted as a function of isoflurane buffer concentration (Figure 1A). The data suggested discrete saturable binding over the isoflurane concentration range tested. At least two binding components, one of higher affinity and one of much lower affinity, were required to adequately describe the data. The ability of oleic acid, an endogenous high-affinity ligand for albumin, to reduce isoflurane binding was examined. Oleic acid, a long-chain fatty acid, was used because of its structural resemblance to the hydrocarbon backbone of long-chain alcohols and alkanes, and because it binds to BSA with very high affinity [dissociation constants in the nanomolar to micromolar range (Spector & Fletcher, 1978)]. It is generally interpreted that a BSA molecule can predominantly bind up to six long-chain fatty acids (Peters, 1985); the structure of these binding sites is becoming increasingly defined (Cistola et al., 1987). Oleic acid was added to BSA at molar ratios (oleic acid/BSA) ranging from 1.5 to 12.0. Isoflurane binding to BSA was measured at an aqueous isoflurane concentration of 3.7 mM. At increasing molar ratios, isoflurane binding was found to progressively decrease (Figure 1B). The reduction was seen to plateau at a molar ratio of 6:1. At a molar ratio of 6:1, isoflurane binding was then characterized (Figure 1A). The binding was markedly reduced by oleic acid, and the residual low-affinity isoflurane binding could be reasonably well fit by a straight line. An oleic acid displaceable, higher affinity isoflurane binding component could be defined by subtracting the isoflurane binding present with oleic acid–BSA from total (fatty acid free) isoflurane binding. The isolated binding was well described by a single equilibrium (K_D = 1.4 ± 0.2 mM, B_{max} = 4.2 ± 0.3 sites) (Figure 1A).

The effect of altered BSA conformation on isoflurane binding was then examined. BSA is known to undergo a large transition in conformation (N–F transition) at low pH (Wishnia & Pinder, 1964). To outline the conformational transition, isoflurane binding to BSA was measured at successively lower pH values, at an isoflurane concentration of 4.4 mM (Figure 1C). Isoflurane binding was found to decrease with decreasing pH. Most of the reduction in binding occurred between pH 5 and pH 3. The reduction in binding leveled off at pH 2.5. These results were very analogous to the (N–F transition) decrease in hydrocarbon binding observed by Wishnia (1964). Isoflurane binding to BSA at pH 2.5 was then characterized. Higher affinity binding was no longer present (Figure 1A). The resultant low-affinity binding was well fit by a straight line. The original higher affinity isoflurane binding could be defined by subtracting the isoflurane binding at pH 2.5 from total isoflurane binding (at pH 7.2). The isolated binding was reasonably well described by a single equilibrium (K_D = 1.1 ± 0.2 mM, B_{max} = 3.3 ± 0.2 sites).

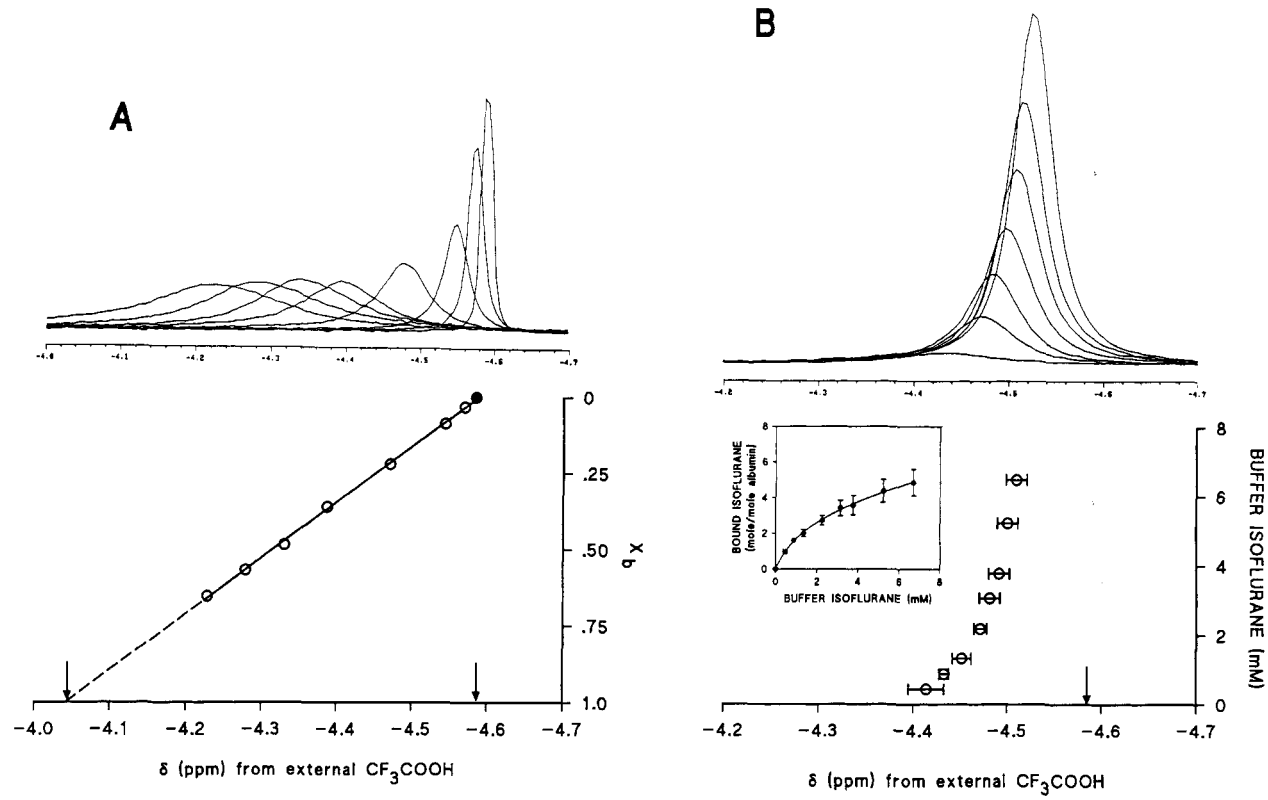

FIGURE 2: (A) Stacked ^{19}F-NMR spectra of the trifluoromethyl group of isoflurane at 470.3 MHz and 22 °C, in buffer (●) and in BSA solutions of (○) 2, 5, 15, 30, 50, 70, and 100 mg/mL, all referenced to CF_3COOH in an external capillary. All samples were equilibrated with 3 vol % isoflurane to give an aqueous concentration of 1.4 mM. X_b was measured for each sample by use of gas chromatographic methods. The chemical shift of isoflurane in buffer is indicated by the right arrow, $\delta_f = -4.585$ ppm. The chemical shift in the bound state is extrapolated to $X_b = 1$ and is given by the left arrow, $\delta_b = -4.042$ ppm. (B) Representative stacked ^{19}F-NMR spectra of the trifluoromethyl group of isoflurane in BSA solution (15 mg/mL) after equilibration with increasing isoflurane (0.5–15 vol %) concentrations. Resulting aqueous concentrations are indicated on the ordinate. The measured chemical shift on the abcissa allowed calculation of X_b and bound isoflurane at each concentration (displayed in inset). More than one equilibrium binding constant were required for a good fit.

The relative specificity of the isoflurane–BSA interaction was next determined by examining isoflurane binding to poly(L-lysine) (MW 114 000), and lysozyme (MW 14 300). In order to detect potential low-affinity binding, a high isoflurane concentration was used. At 11.4% gaseous isoflurane, which yields a buffer isoflurane concentration of 5.2 ± 0.3 mM, poly(L-lysine) [27.8 mg/mL (0.24 mM)] and lysozyme [27.8 mg/mL (1.94 mM)] produced total solution isoflurane concentrations of 5.4 ± 0.2 and 5.1 ± 0.3 mM, respectively. Both protein solution isoflurane concentrations are not significantly different from buffer isoflurane. The minimal binding to poly(L-lysine) and lysozyme indicates specificity in isoflurane interaction with macromolecules.

^{19}F-NMR Chemical Shift Analysis of Isoflurane Equilibrium Binding at pH 7.2. The isoflurane trifluoromethyl chemical shift in buffer was observable as a single ^{19}F-NMR resonance (unresolvable doublet) at –4.585 ± 0.003 ppm referenced to external trifluoroacetic acid (Figure 2A). The chemical shift was shown to be independent of isoflurane concentration. The bound trifluoromethyl chemical shift, δ_b, was measured by observing the influence of BSA on the chemical shift. This was done by equilibrating BSA samples, ranging from 2.0 to 100 mg/mL, with 2.8% isoflurane, giving samples an aqueous isoflurane concentration of 1.41 mM. Spectra were collected and consisted of a single trifluoromethyl chemical shift, which progressively shifted to lower field as a function of increasing protein concentration (Figure 2A). From gas chromatographic partition measurements also made at 1.41 mM aqueous isoflurane, X_b, the bound anesthetic mole fractions, were determined for the samples. The observed chemical shift, δ, was found to correlate linearly with X_b. The observation demonstrated that isoflurane was rapidly exchanging between bound and free environments. It followed then that the observed chemical shift, δ, represented a weighted average of the isoflurane chemical shift in aqueous solution and bound to BSA. Expressed mathematically (Dwek, 1973)

$$\delta = X_b\delta_b + X_f\delta_f \quad (7)$$

where δ_b is the bound trifluoromethyl chemical shift, δ_f is the free trifluoromethyl chemical shift –4.585 ppm, and $X_b + X_f = 1$. Equation 7 describes the linear relation of Figure 2A. When $X_b = 1$, $\delta = \delta_b = -4.042$ ppm, which is the extrapolated intercept. The resulting chemical shift between free and bound anesthetic, $\delta\omega = \delta_b - \delta_f = 0.545$ ppm.

To investigate whether δ_b was uniform over the entire isoflurane concentration range, BSA solutions (15 mg/mL) were equilibrated with varying isoflurane concentrations (1.0–15 vol %). At 0.44 mM isoflurane, the chemical shift was observed at –4.409 ± 0.01 ppm. With increasing isoflurane concentrations, the resulting chemical shift shifted toward $\delta_f = -4.585$ ppm (Figure 2B). This was expected with increasing aqueous isoflurane concentration, because X_b progressively decreased (and X_f increased) as the limited number of higher affinity binding sites became occupied. A uniform value for δ_b (–4.042 ppm.) was used in order to calculate bound isoflurane from the observed chemical shift values at various isoflurane concentrations [Figure 2B (inset)]. The bound isoflurane measurements were in reasonable agreement with the gas chromatographic measurements and clearly required at least two separate components to describe the binding. A high-affinity component, similar to that derived from the gas

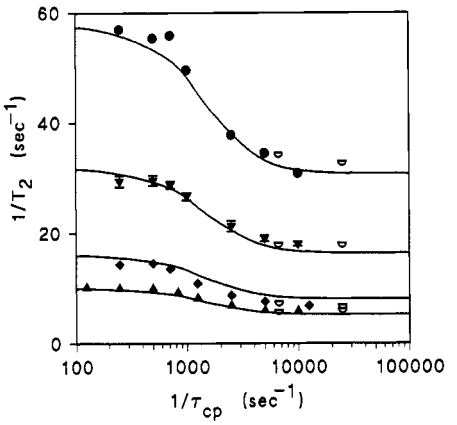

FIGURE 3: Observed transverse relaxation rate, $1/T_2$, of the trifluoromethyl group of isoflurane in BSA solutions at 22 °C plotted as a function of pulsing rate ($1/\tau_{cp}$). Four different values of X_b were used: 0.19 (●), 0.10 (▼), 0.048 (◆), 0.028 (▲). Each data set was separately fit to eq 4, adjusting $\delta\omega$, τ_b, and T_{2b}, until a good fit was found. The resulting averages, $\delta\omega$ = 0.34 ppm, τ_b = 0.184 ms, and T_{2b} = 6.3 ms, were used to draw solid curves through all the data sets. Spin-locking relaxation rates were determined at locking field frequencies of 3333 and 12 500 Hz. The measured relaxation rates (ᴗ) are plotted as a function of the CPMG pulsing equivalent of these locking field frequencies.

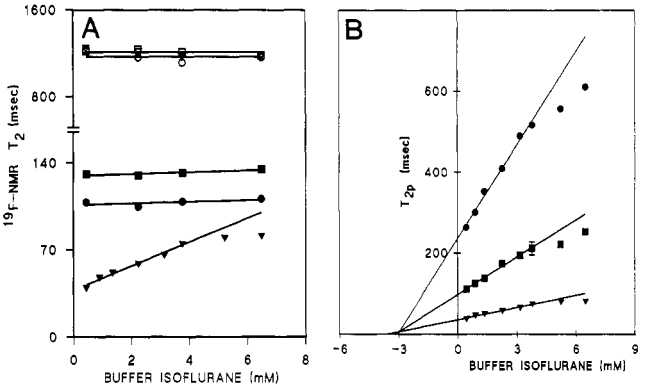

FIGURE 4: (A) ^{19}F-NMR isoflurane trifluoromethyl T_2 measured using a fast CPMG pulsing rate ($1/\tau_{cp}$ = 10 000 s^{-1}) and plotted as a function of aqueous isoflurane, for BSA (6 mg/mL) (▼), BSA (6 mg/mL) in the presence of oleic acid (6:1 oleic acid/BSA mole ratio) (●), BSA (6 mg/mL) at pH 2.5 (■), lysozyme (6 mg/mL) (□), poly(L-lysine) (6 mg/mL) (○), and buffer alone (▽). (B) ^{19}F-NMR isoflurane trifluoromethyl T_{2p} measured for BSA at three different concentrations: 6 (▼), 1.75 (■), and 0.75 mg/mL (●).

chromatographic data (K_D = 1.4 mM, B_{max} = 3.1 sites), was fit with a lower affinity binding component to describe the data. Since the chemical shift analysis relied on gas chromatographic measurements to determine δ_b, it did not represent an independent measurement of bound isoflurane. The analysis did indicate, however, that the chemical shift of the lower affinity isoflurane binding was similar to the chemical shift of the higher affinity isoflurane binding, such that one uniform δ_b was able to describe the binding reasonably well.

^{19}F-NMR T_2 Analysis of Isoflurane Equilibrium Binding. The trifluoromethyl T_2 relaxation of isoflurane in buffer, and in BSA solution, was strictly uniexponential for all concentrations and all CPMG pulsing rates indicated in this study. In buffer, $1/T_2 = 0.83 \pm 0.03$ s^{-1} and did not vary as a function of the CPMG 180–180° interpulse space interval (τ_{cp}). When BSA was added, however, $1/T_2$ was found to systematically decrease with decreasing τ_{cp}. The relationship between pulsing rate, $1/\tau_{cp}$, and relaxation rate, $1/T_2$, was examined at four different values for X_b: 0.19, 0.10, 0.048, and 0.028 (Figure 3). At all four values of X_b, relaxation rates decreased to a constant value as the pulsing rate was increased. The data sets were separately fit to eq 4. The average values $\delta\omega = 0.34 \pm 0.01$ ppm, $\tau_b = 184 \pm 11$ μs, and $T_{2b} = 6.3 \pm 0.5$ ms, were used to draw solid curves through all data sets (Figure 3). The value $\delta\omega$ = 0.34 ppm was in reasonable agreement with the experimentally determined $\delta\omega$ = 0.545 ppm. To determine if the fast pulsing rate minimized the time allowed for isoflurane exchange, and hence, minimized the exchange process contribution, a spin-lock experiment was performed in each of the four cases. The objective was to perform the experiment at a locking field frequency that was the locking equivalent of a fast CPMG pulsing rate (Santyr et al., 1988). Relaxation rates obtained in the spin-lock experiments were compared to those acquired using the equivalent CPMG pulsing rate. Two locking field frequencies were chosen, 3333 and 12 500 Hz, which corresponded to CPMG pulsing rates of 6666 and 25 000 Hz. Virtually identical relaxation rates were measured by the spin-lock experiment and the fast CPMG pulsing rate experiments (Figure 3).

The dependence of the observed T_2 on isoflurane concentration was examined using a fast CPMG pulsing rate, $1/\tau_{cp}$ = 10 000 s^{-1}. In buffer, T_2 = 1210 ± 40 ms and showed no dependence on isoflurane concentration (Figure 4A). In BSA solution (6 mg/mL), a strong isoflurane concentration dependence was evident. Since the fast pulsing rate eliminated chemical exchange contributions to relaxation, the observed T_2 simply reflected the weighted average of the trifluoromethyl relaxation rates in the bound and free states (eq 2). At 0.44 mM aqueous isoflurane, T_2 = 38 ± 1 ms. When isoflurane concentration was increased to 6.4 mM, T_2 increased to 75 ± 2 ms. The increase in the observed T_2 was expected with increasing aqueous isoflurane concentration, because X_b decreased (and X_f increased) as the limited number of higher affinity binding sites became occupied (analogous to the chemical shift demonstration). When isoflurane binding to BSA (6 mg/mL) was analyzed in the presence of oleic acid (mole ratio of 6:1), there was virtually no change in T_2 with increasing isoflurane concentration (Figure 4A). At 0.44 mM isoflurane, T_2 = 108 ± 2 ms and increased only to 111 ± 2 ms at 6.49 mM isoflurane. This was expected in the case of lower affinity binding, since X_b changed very little when binding sites could not appreciably fill over the isoflurane concentration range. Isoflurane binding to BSA at pH 2.5 was similarly expected to show little T_2 dependence on isoflurane concentration. Indeed, only a minimal change in T_2 was seen; at 0.44 mM isoflurane, T_2 = 130 ± 2 ms and increased to 135 ± 1 ms at 6.49 mM isoflurane (Figure 4A).

Isoflurane binding to BSA (pH 7.2) represented a significant immobilization of anesthetic molecules as revealed by T_{2b}. Based on eq 4, a T_{2b} = 6.3 ± 0.5 ms and τ_b = 184 ± 11 μs were calculated. The lower affinity isoflurane binding, observed in the presence of oleic acid, and at pH 2.5, also represented significant anesthetic immobilization. Based on eq 4, values for T_{2b} equal to 9.2 and 10.2 ms were calculated. Values for τ_b equal to 70 and 60 μs were also calculated in the presence of oleic acid, and at pH 2.5. The lower affinity binding represented a marked decrease in τ_b. Negligible interactions of isoflurane with poly(L-lysine (6 mg/mL) and lysozyme (6 mg/mL) were demonstrated by the observed T_2 values of 1210 ± 30 and 1170 ± 50 ms, which were virtually identical to buffer (1210 ± 40 ms) (Figure 4A).

For BSA concentrations of 6, 1.75, and 0.75 mg/mL, T_{2p} was plotted as a function of isoflurane concentration (Figure 4B). T_{2p} was calculated, $T_{2p} = (1/T_2 - 1/T_{2f})^{-1}$, where T_{2f} equaled the observed isoflurane T_2 in buffer. An x-intercept

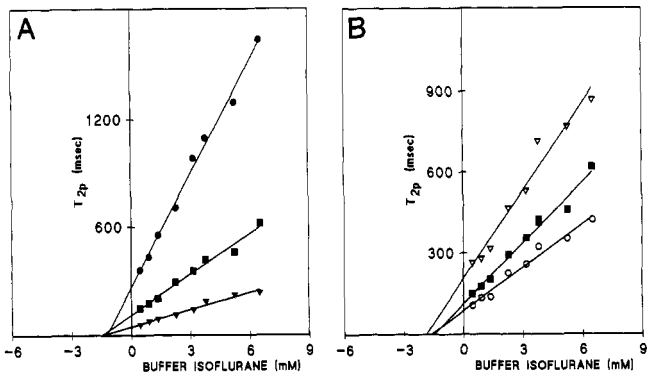

FIGURE 5: (A) ^{19}F-NMR isoflurane trifluoromethyl T_{2p}, measured for BSA at three different concentrations: 6 (▼), 1.75 (■), and 0.75 mg/mL (●). T_{2p} was calculated using the T_2 of isoflurane in oleic acid–BSA as T_{2f}. In this way, the higher affinity isoflurane binding was isolated. Note the linearity of the plot, indicative of a single equilibrium, and an x-intercept K_D = 1.4 mM. (B) ^{19}F-NMR isoflurane trifluoromethyl T_{2p} in BSA solution (1.75 mg/mL) plotted at three different temperatures: 6 (○), 22 (■), and 38 °C (▽). The equilibrium binding constant, as measured by the x-intercept, was relatively temperature insensitive.

was drawn through the linear portion of each data set. A deviation from linearity was expected because of the presence of more than a single binding component as indicated by gas chromatography. The indicated x-intercept does not solely reflect the higher affinity binding component since the lower affinity binding is necessarily affecting T_{2p} values at all isoflurane concentrations. In order to outline the higher affinity binding, the lower affinity binding had to be observed in isolation, as described, for example, using oleic acid (6:1 oleic acid/BSA mole ratio) (Figure 4A). The measured T_2 values in oleic acid–BSA solution at 6, 1.75, and 0.75 mg/mL were substituted for T_{2f} in the calculation of T_{2p}. The modified T_{2p} values were replotted (Figure 5A). The modified T_{2p} values reflect solely the higher affinity, oleic acid displaceable binding. Linearity was expected because the oleic acid displaceable binding was well described by a single equilibrium by gas chromatography. An x-intercept K_D = 1.4 mM was in excellent agreement with the gas chromatographically defined higher affinity binding. Isoflurane binding to BSA at pH 2.5 was alternatively used to outline the higher affinity binding. The T_2 plots linearized as expected, yielding an x-intercept K_D = 1.3 mM (not shown).

T_{2b} increases and τ_b decreases for a rapidly exchanging system when the temperature is increased (Sykes et al., 1970; Dwek, 1973). Since $T_{2b} \gg \tau_b$, T_{2b} was expected to be the dominant factor in the slope, $(T_{2b} + \tau_b)/[R]$. Therefore, at a given BSA concentration, the slope was expected to increase with increasing temperature. To verify this, the isoflurane concentration dependence of T_{2p} was measured for BSA (1.75 mg/mL) at 6, 22, and 38 °C. The slopes were indeed found to increase with increasing temperature (Figure 5B). Since T_{2b} = 6.3 ms at 22 °C, values for T_{2b} = 4.5 at 6 °C and T_{2b} = 9.1 ms at 38 °C could be calculated based on the ratio of the slopes.

DISCUSSION

The goal of this study was to directly assess the ability of fluorinated volatile anesthetics to discretely bind to protein molecules and, further, to directly characterize the binding affinities. The ability to observe and characterize volatile anesthetic binding to protein is essential for evaluating the molecular mechanisms through which volatile anesthetics act.

The methods used to characterize volatile anesthetic binding were based on analysis of ^{19}F-NMR T_2 relaxation. The use of T_2 relaxation (or line broadening) to characterize equilibrium binding of ligands to macromolecules has been developed and applied (Fischer & Jardetzky, 1965; Schmidt et al., 1969) in several other systems. Generally, application of these methods has been limited to situations in which chemical shift differences between bound and free ligand do not contribute to the observed T_2. The minor modification of measuring T_2 using rapid pulsing in a CPMG sequence (effecting a spin lock) allowed us to apply T_2 methods to volatile anesthetic binding to albumin, a situation in which there is a significant chemical shift difference between bound and free ligand.

The high-affinity component of volatile anesthetic binding to albumin was isolated by use of a pharmacologic displacer. This same approach has previously been described for the NMR measurement of cholinergic agonist binding to the nicotinic acetylcholine receptor (Miller et al., 1979; Behling et al., 1988). There are no known displacers for volatile anesthetic binding. For albumin, oleic acid (a long-chain fatty acid) and a pH alteration of conformation were effective in "displacing" higher affinity isoflurane binding. Importantly, other selected volatile and general anesthetics were also effective in displacing higher affinity isoflurane binding to BSA (manuscript in preparation).

The measured lifetime of isoflurane in the BSA bound state, τ_b = 184 μs, yields information about lifetimes in both the higher and lower affinity binding states. For the measured samples, higher affinity sites represented approximately 63% of total binding. The lifetime in the lower affinity sites was observed in isolation using oleic acid or pH 2.5. Values of τ_b = 70 μs and τ_b = 60 μs were measured. Assuming that the higher and lower affinity sites are independent, a τ_b = (184 − 0.37(70))/0.63 = 251 μs can be calculated for the higher affinity sites. The dissociation constant, K_D, of the higher affinity sites equals k_{off}/k_{on} = 1.4 mM. $k_{off} = 1/\tau_b$ = 3984 s^{-1} and allows a determination of $k_{on} = 2.8 \times 10^6$ M^{-1} s^{-1}.

The clinical concentration of isoflurane required for anesthesia is approximately 0.3 mM (Firestone et al., 1986). It is remarkable that BSA, a protein that clearly has no mechanistic role in anesthesia, binds isoflurane with an affinity (K_D = 1.4 mM) only slightly out of the clinical range. This demonstrates that the NMR T_2 relaxation method will be useful in analyzing anesthetic binding to other purified proteins in the clinical concentration range. It is also interesting to speculate that the fatty acid binding domains on BSA are somewhat relevant and bare some resemblance to putative pockets on neuronal ion channels. Indeed, recent evident has demonstrated the ability of fatty acids, (and arachidonate metabolites) to *directly* regulate certain neuronal and smooth muscle ion channel function (Hwang et al., 1990; Ordway et al., 1991)).

In summary, this paper provides *direct* evidence that distinct fluorinated volatile anesthetic binding sites exist on certain proteins, in certain conformations, and provides a sensitive method to describe them.

ACKNOWLEDGMENT

We thank D. Andre d'Avignon for assistance in pulse programming and Doug Covey and David Cistola for comments on the manuscript.

REFERENCES

Alifimoff, J. K., Firestone, L. L., & Miller, K. W. (1989) *Br. J. Pharmacol. 96*, 9.

Allerhand, A., & Gutowsky, H. S. (1965) *J. Chem. Phys. 42*, 1587.
Balasubramanian, D., & Wetlaufer, D. B. (1966) *Proc. Natl. Acad. Sci. U.S.A. 55*, 762.
Behling, R. W., Yamane, T., Navon, G., & Sammon, M. J. (1988) *Biophys. J. 53*, 947.
Bovey, F. A. (1988) *Nuclear Magnetic Resonance Spectroscopy*, pp 255–321, Academic Press, San Diego, CA.
Brown, F. F., Halsey, M. J., & Richards, R. E. (1976) *Proc. R. Soc. London B 193*, 387.
Carver, J. P., & Richards, R. E. (1972) *J. Magn. Reson. 6*, 89.
Cistola, D. P., Small, D. M., & Hamiltion, J. A. (1987) *J. Biol. Chem. 262*, 10971.
Dwek, R. A. (1973) *Nuclear Magnetic Resonance in Biochemistry*, pp 37–47, Clarendon Press, Oxford, England.
Firestone, L. L., Miller, J. C., & Miller, K. W. (1986) in *Molecular and Cellular Mechanisms of Anesthetics* (Roth, S. H., & Miller, K. W., Eds.) pp 455–470, Plenum, New York.
Fischer, J. J., & Jardetzky, O. (1965) *J. Am. Chem. Soc. 87*, 3237.
Fraenkel, Y., Navon, G., Aronheim, A., & Gershoni, J. M. (1990) *Biochemistry 29*, 2617.
Franks, N. P., & Lieb, W. R. (1984) *Nature 310*, 599.
Franks, N. P., & Lieb, W. R. (1987) *Nature 316*, 349.
Franks, N. P., & Lieb, W. R. (1991) *Science 254*, 427.
Gerig, J. T., & Stock, A. D. (1975) *Org. Magn. Reson. 7*, 249.
Gerig, J. T., Halley, B. A., & Ortiz, C. E. (1977) *J. Am. Chem. Soc. 99*, 6219.
Hartmann, S. R., & Hahn, E. L. (1962) *Phys. Rev. 128*, 2042.
Heavner, J. E., Friedhoff, J., & Haschke, R. (1976) *Anesthesiology 45*, 654.
Hills, B. P., Takacs, S. F., & Belton, P. S. (1989) *Mol. Phys. 67*, 903.
Hills, B. P., Takacs, S. F., & Belton, P. S. (1990) *Food Chem. 37*, 95.
Hwang, T. C., Guggino, S. E., & Guggino, W. B. (1990) *Proc. Natl. Acad. Sci. U.S.A. 87*, 5706.
Jackman, J. M., & Cotton, F. A. (1975) *Dynamic Nuclear Magnetic Resonance Spectroscopy*, pp 145–149, Academic Press, New York.
Laasberg, L. H., & Hedley-Whyte, J. (1970) *Anesthesiology 32*, 351.
Laasberg, L. H., & Hedley-Whyte, J. (1971) *J. Biol. Chem. 246*, 4886.
Luz, Z., & Meiboom, S. (1963) *J. Chem. Phys. 39*, 366.
Mashimo, T., Kamaya, H., & Ueda, I. (1986) *Mol. Pharmacol. 29*, 149.
Meiboom, S., & Gill, D. (1958) *Rev. Sci. Instrum. 29*, 688.
Miller, J., Witzemann, V., Quast, U., & Raftery, M. A. (1979) *Proc. Natl. Acad. Sci. U.S.A. 76*, 3580.
Ordway, R. W., Singer, J. J., & Walsh, J. V., Jr. (1991) *Trends Neurosci. 14*, 96.
Peters, T. (1985) *Adv. Protein Chem. 37*, 161.
Ray, A., Reynolds, J. A., Polet, H., & Steinhardt, J. (1966) *Biochemistry 5*, 2606.
Richards, C. D., Martin, K., Gregory, S., Keightley, C. A., Hesketh, T. R., Smith, G. A., Warren, G. B., & Metcalfe, J. C. (1978) *Nature 276*, 775.
Santyr, G. E., Henkelman, R. M., & Bronskill, M. J. (1988) *J. Magn. Reson. 79*, 28.
Schmidt, P. G., Stark, G. R., & Baldeschwieler, J. D. (1969) *J. Biol. Chem. 244*, 1860.
Spector, A. A. (1986) *Methods Enzymol. 128*, 320.
Spector, A. A., & Fletcher, J. E. (1978) in *Disturbances in Lipid and Lipoprotein Metabolism* (Dietschy, J. M., Gotto, A. M., & Ontko, J. E., Eds.) pp 229–248, American Physiological Society, Bethesda, MD.
Stern, R. C., Towler, S. C., White, P. F., & Evers, A. S. (1990) *Anesth. Analg. 71*, 658.
Swift, T. J., & Connick, R. E. (1962) *J. Chem. Phys. 37*, 307.
Sykes, B. D., Schmidt, P. G., & Stark, G. R. (1970) *J. Biol. Chem. 245*, 1180.
Wishnia, A. (1962) *Proc. Natl. Acad. Sci. U.S.A. 48*, 2200.
Wishnia, A., & Pinder, T. (1964) *Biochemistry 3*, 1377.